HADRONIC FINAL STATES IN SOFT PHOTON-PHOTON SCATTERING

Hermann Kolanoski

Physikalisches Institut der Universität Bonn
Federal Republic of Germany

Abstract

In this talk experimental results on the non-resonant production of hadrons in soft $\gamma\gamma$ scattering are reviewed:
The measured cross sections for the production of hadron pairs by two photons are compared to theoretical predictions (QCD calculations above about 2 GeV).
Analyses of four pion final states are reported, including an angular correlation analysis of $\rho^0\rho^0$, first results on $\rho^+\rho^-$ production and the observation of a narrow structure in the four pion mass spectrum near 2.1 GeV.
The experimental results on the total hadronic cross section for photon-photon scattering are critically discussed.

1.0 INTRODUCTION

The title of this talk raises the very general question: How do the photons turn into hadrons? However, I will not be all that general. Since this is a review of the experimental status, the framework for the talk is given by the results available on hadronic final states in soft $\gamma\gamma$ scattering. "Soft" is meant to distinguish this talk from the talk given by N.Wermes at this workshop on hard scattering phenomena such as jet production by two photons and from the talk given by W.Wagner on deep inelastic electron-photon scattering involving high Q^2 values of the photons. The experimental aspects of resonance production by two photons are reviewed by J.Olsson at this workshop.

This talk will cover three topics:

- Two-photon production of hadron pairs.
- Two-photon production of four pions.
- The total cross section for two-photon production of hadrons (concentrating on the low energy, low Q^2 region).

2.0 HADRON PAIR PRODUCTION BY TWO PHOTONS

I will begin with summarizing our knowledge about the continuum production of hadron pairs at low energies. The understanding of these reactions is important for the analysis of two-photon production of resonances decaying into hadron pairs. One cannot always get rid of the background from the continuum by a simple subtraction, but interferences between resonances and continuum may also change the resonance shapes.

In the second part of this chapter new results on hadron pair production for $\gamma\gamma$ invariant masses ($W_{\gamma\gamma}$) above 2 GeV are presented. The experimental results will be compared to QCD calculations.

2.1 HADRON PAIR PRODUCTION AT LOW ENERGIES

In the resonance region most experimental information is available on the $\pi^+\pi^-$ continuum which will be discussed in more detail below.

The $\pi^\circ\pi^\circ$ continuum below ~1 GeV has not yet been analyzed, though data are available from the JADE experiment. This channel may be best suited to look for broad $\pi\pi$ resonances below ~1 GeV.

The reaction $\gamma\gamma \to K\bar{K}$ has been measured by the TASSO group for the K^+K^- and $K^0_S K^0_S$ final states /1/. The $K\bar{K}$ mass spectra have been used to determine the $\gamma\gamma$-width of the f' (see J.Olsson's talk). A more general analysis of the spectra

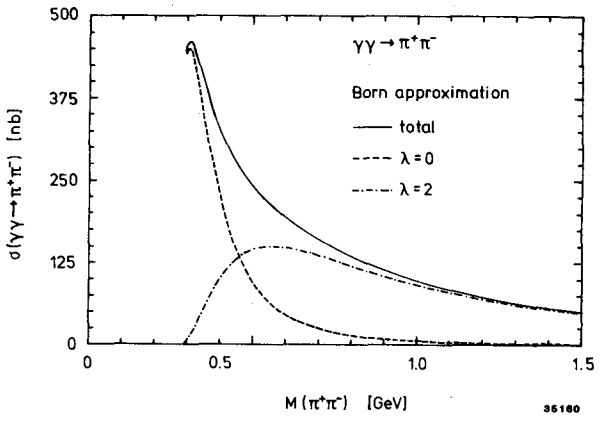

Figure 1. $\sigma(\gamma\gamma\to\pi^+\pi^-)$ (Born): curves for $\gamma\gamma$-helicities 0, 2 and sum of both

including both resonances and continuum is desireable because it would reduce the systematic error on the $\gamma\gamma$-width. A model which describes continuum and resonances by unitarizing the combined scattering amplitude is given in /2/.

2.1.1 The Reaction $\gamma\gamma\to\pi^+\pi^-$ Near Threshold

At low energies the measured cross section for $\gamma\gamma\to\pi^+\pi^-$ may be compared to the Born approximation for this process given by the following graphs:

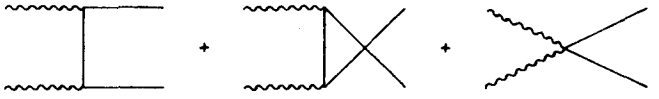

The resulting cross section as well as its decomposition into $\gamma\gamma$-helicity components is shown in Figure 1. When searching for a broad resonance below ~1 GeV, as for the expected scalar meson $\varepsilon(\sim 700)$, a first step in the analysis should be a quantitative comparison of the results with the expectations from a pure Born cross section.

The process $\gamma\gamma\to\pi^+\pi^-$ has been measured at the DCI storage ring in the $\pi\pi$ mass range from threshold to about 0.7 GeV /3/. The pion pairs have been separated from the electron and muon pair background by determining the particle mass from a kinematical reconstruction of the event. With such a method for $\pi\pi$ detection near threshold this experiment is superior to experiments at PETRA or PEP. Unfortunately the experiment suffers from lack of statistics. The measured cross section (within the acceptance) of $\sigma(\gamma\gamma\to\pi^+\pi^-) = 69\pm15$ pb has to be compared to 34 pb for the Born approximation. The difference is only 2.3 standard deviations, not enough to establish a resonance in this region. At present, more data are being collected /4/.

2.1.2 The Reaction $\gamma\gamma \to \pi^+\pi^-$ in the f^0-Region

In Figure 1 we see that the $\gamma\gamma$-helicity 0 contribution to the Born cross section dies out very fast above threshold. In the region of the f^0 resonance helicity 2 is virtually the only contribution. Below the f^0-resonance strong interactions are expected to have only a small effect on the helicity 2 amplitude because the $\pi\pi$ phase shifts are small for $\pi\pi$ angular momenta $J \geq 2$. Therefore it has been suggested that the Born approximation should be a good description of $\gamma\gamma \to \pi^+\pi^-$ as far above threshold as $W_{\gamma\gamma} \sim 1$ GeV (see e.g. /5/). Hence we may compare the data in the f^0-region with an approximation obtained from the Born terms plus a resonance contribution as given by the following graphs:

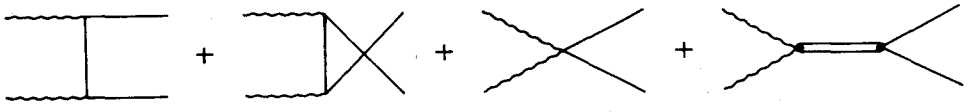

If the resonance is also dominantly produced via helicity 2 a strong interference between the Born graphs and the resonance is expected. The interference is completely determined by the Breit-Wigner phase (the Born amplitude is purely real) except for a relative sign between the Born and the resonance amplitudes. Curves for the two choices of sign are shown in Figure 2.

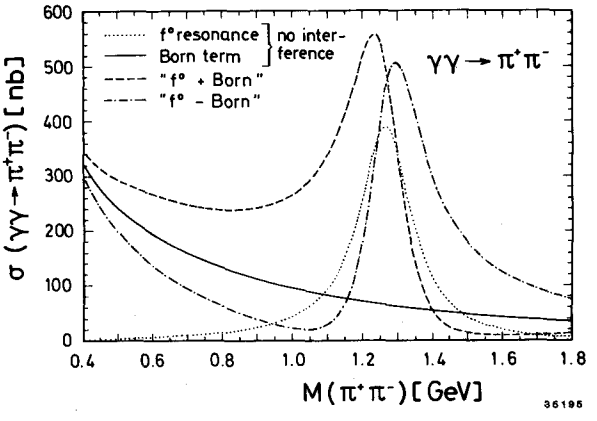

Figure 2. Cross section for the two-photon production of the f^0 (assuming $\lambda=2$) and $\pi^+\pi^-$-continuum : without interference (dotted and full curve), resonance and Born amplitudes interfering with a positive relative sign (dashed curve) and with a negative relative sign (dotted curve).

The justification for such a simple approach is given by the data. Figure 3 shows the $\pi^+\pi^-$-mass spectrum obtained by the Mark II collaboration at SPEAR /6/. The data are compared to calculations for the Born term and the f^0-resonance. Com-

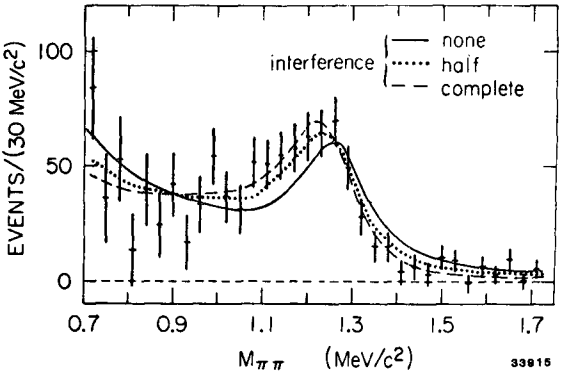

Figure 3. Mark II: Invariant mass of events with two charged tracks assigning pion masses to all tracks, QED background subtracted.

plete interference, which is expected if the f^0 is produced mainly via helicity 2, gives a good description of the data.

New data from the CELLO group exhibit the same structure in the $\pi^+\pi^-$-mass spectrum (Figure 4) /7/. This spectrum was obtained selecting two oppositely charged tracks with $|\cos\Theta|<0.8$ and transverse momenta w.r.t. the beam $p_T>0.35$ GeV/c. The resulting transverse momentum of the two particles was required to be smaller than 0.1 GeV/c. Since the pions have not been identified, the electron and muon pairs from the QED processes had to be subtracted.

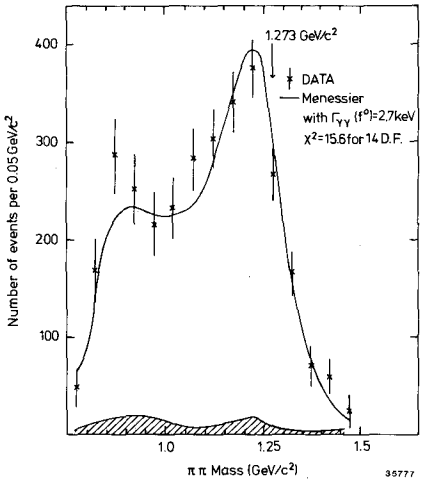

Figure 4. CELLO: Invariant mass of events with two charged tracks assigning pion masses to all tracks, QED background subtracted. The hatched area is the estimated K^+K^- background. The solid curve is explained in the text.

The CELLO results on $\pi^+\pi^-$ production between 0.8 and 1.5 GeV are well described by a model of Mennessier /2/ (solid curve in Figure 4). In this model the amplitudes for a given partial wave and given isospin are composed of a unitarized Born term, a unitarized term for vector exchange and terms describing the direct couplings of the photons to resonances. In the CELLO analysis only the unitarized Born term and the coupling to the f^0-resonance were necessary. In particular, a contribution of a scalar resonance was not required by the data. The modification of the Born term obtained from the unitarization procedure using strong interaction data turns out to be small /7/. This may be due to the smallness of the D-wave phase shifts below the f^0-mass.

The status of the analysis of the $\gamma\gamma$-width of the f^0 was reviewed by J.Olsson at this workshop.

2.2 PRODUCTION OF PROTON-ANTIPROTON PAIRS

The TASSO collaboration published an analysis of the reaction $\gamma\gamma \to p\bar{p}$ based on 8 observed events /8/. This analysis has now been repeated with much higher integrated luminosity ($\sim 74 pb^{-1}$) increasing the number of events by an order of magnitude /9/.

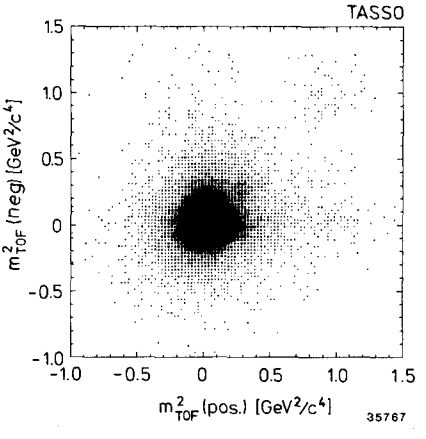

Figure 5. Square of the mass calculated from TOF for the negative track vs. the same quantity for the positive track in an event with 2 charged tracks detected

Candidate events for the reaction $\gamma\gamma \to p\bar{p}$ have been selected from events with two oppositely charged tracks in a polar angular range $|\cos\Theta| < 0.8$ and in a momentum range $0.35 \leq p \leq 1.6$ GeV/c. The $p\bar{p}$ pairs have been identified by means of the time-of-flight (TOF) information of the counters surrounding the TASSO central drift chamber. In Figure 5 the square of the mass calculated from TOF for the positive track is plotted versus the same quantity for the negative track. The cluster of $p\bar{p}$ events is clearly separated. The final sample contains 72 $p\bar{p}$ events

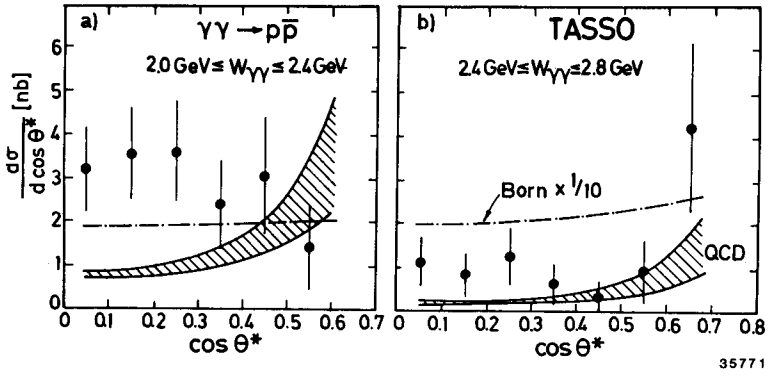

Figure 6. $d\sigma/d\cos\Theta^*$ for $\gamma\gamma \to p\bar{p}$: a) $2.0 < W_{\gamma\gamma} < 2.4$ GeV and b) $2.4 < W_{\gamma\gamma} < 3.0$ GeV. Data are compared to the Born approximation for a Dirac proton (dashed-dotted curve, scaled by 1/10) and to QCD calculations /11/ (hatched area). The band for the QCD calculations corresponds to different choices for the parton distribution in the protons.

with invariant masses between 2.0 and 3.1 GeV and with $|\sum \vec{p}_T| < 0.1$ GeV/c ($|\sum \vec{p}_T|$ is the transverse momentum of the detected system w.r.t. the beam). The background contributes less than 5 events.

In Figure 6 the differential cross section for $\gamma\gamma \to p\bar{p}$ as a function of $|\cos\Theta^*|$ (Θ^* = polar angle of the p in the $\gamma\gamma$ rest system) is given for two $p\bar{p}$-mass intervals. In both intervals the differential cross section is consistent with a flat $\cos\Theta^*$ dependence. The differential cross section averaged over the accepted Θ^* range is plotted in Figure 7 as a function of the $p\bar{p}$-mass. The measured differential cross

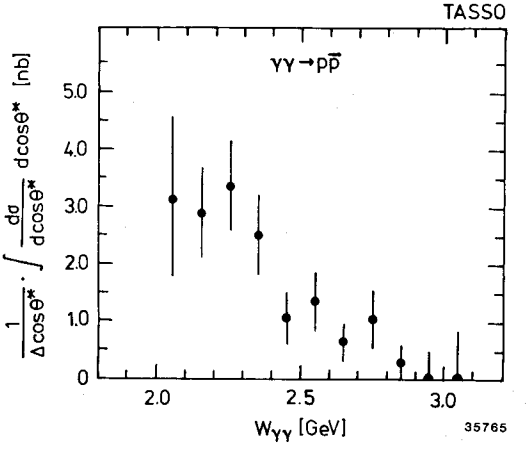

Figure 7. $d\sigma/d\cos\Theta^*$ for $\gamma\gamma \to p\bar{p}$, averaged over the accepted angular range, as a function of the $p\bar{p}$ mass.

sections are compared to the Born approximation for the process $\gamma\gamma \to p\bar{p}$ assuming Dirac protons (dashed-dotted curve, scaled by 1/10). This approximation is an order of magnitude too large. Including the anomalous magnetic moment of the proton yields even higher cross sections /10/.

The results are also compared to an absolute QCD calculation done by Damgaard /11/ with methods developed by Brodsky and Lepage /12/ (see also the discussion in Stirling's talk at this workshop). Although these calculations are meant to be meaningful only at higher energies, above about 3 GeV, one finds that the extrapolation of the predictions to below 3 GeV yields cross sections of the same order of magnitude as the experimental results. In the QCD calculations it is assumed that, if a high momentum transfer is involved in the scattering process, the scattering amplitude factorizes into a hard scattering amplitude T_H and a parton distribution function Φ:

$$M \sim \Phi^* \cdot T_H \cdot \Phi$$

The soft part, the parton distribution function Φ, cannot be calculated. For the form of parton distribution one has to make reasonable assumptions. The absolute normalisation of Φ is then obtained by comparing with other processes containing the same distribution function (in this case $J/\Psi \to p\bar{p}$). The hard scattering amplitude T_H can be calculated perturbatively by evaluating QCD diagrams. In /11/ the differential cross section for $p\bar{p}$ production was calculated for $W_{\gamma\gamma} = M_{J/\Psi}$. An extension to other energies is obtained from the dimensional counting rule according to:

$$\frac{d\sigma}{dt} = \frac{1}{s^6} f(t)$$

Here s,t are the usual Mandelstam variables for the process $\gamma\gamma \to p\bar{p}$. The function f(t) strongly rises towards the forward direction. This behaviour has not yet been observed in the data, but it is also not excluded. On the other hand, the QCD calculations are most reliable at large angles where the measurements have been done.

2.3 HADRON PAIR PRODUCTION ABOVE 2 GEV

The PLUTO group looked for charged hadron pairs with invariant masses above 2 GeV not separating pions, kaons and protons /13/. An earlier analysis yielded upper limits /14/. The new analysis uses data from ~40 pb^{-1}. The charged hadrons have not been explicitly identified, but were defined as not being electron or muon pairs. Since the QED processes are by far dominant, this procedure requires an excellent rejection probability for electrons and muons. That has been achieved using the barrel shower counters and the muon detection system of the PLUTO detector. Events with two oppositely charged tracks with $|\cos\Theta|<0.6$ and momenta larger than 0.9 GeV/c were selected. The photons were restricted to have low Q^2 values by the requirement that there was no tag in the small and large angle taggers. Exclusively produced pairs were selected by demanding

$|\sum \vec{p}_T| < 0.5$ GeV/c and that the tracks were coplanar with the beam within 6°. The process $\gamma\gamma \to e^+e^-$ has been rejected by a cut in the shower energies leading to about 20% loss of hadron pairs but virtually no remaining background from electrons. The remaining 987 events are mainly events from the reaction $\gamma\gamma \to \mu^+\mu^-$ with a small contribution from hadron pair production.

For the separation of the hadron pairs from the muons it was demanded that the particles should have momenta and angles such that if they were μ's they could be identified with a probability greater than 98%. 651 events fulfilled this requirement. Only 16 of them were not identified as $\mu^+\mu^-$. After subtraction of the estimated $\mu^+\mu^-$ background 15.1 hadron pair events were left yielding the ratio of hadron pair production to muon pair production:

$$\frac{\sigma(e^+e^- \to e^+e^-h^+h^-)}{\sigma(e^+e^- \to e^+e^-\mu^+\mu^-)} (W_{\pi\pi} > 2.0 \text{ GeV}) = 0.042 \pm 0.013(\text{stat.}) \pm 0.008(\text{syst.})$$

This result is more than an order of magnitude smaller than expected for a pointlike production of hadrons, but it is in reasonable agreement with the QCD calculations of /12/ which predict for this ratio 0.020 ± 0.001. In Figure 8 the ratio of the two-photon produced hadron pairs to muon pairs is plotted versus the mass of the hadron pair assuming pion masses for all hadrons. The lowest $\pi\pi$ mass of 2 GeV corresponds to a KK-mass of 2.21 GeV and a $p\bar{p}$ mass of 2.73 GeV. The QCD calculation suggests that the hadron composition within the acceptance is 48% $\pi^+\pi^-$, 48% K^+K^- and 4% $p\bar{p}$. The QCD curve in Figure 8 was obtained with this composition assuming pion masses for all particles as in the data.

In conclusion, in this analysis and in the TASSO analysis of $\gamma\gamma \to p\bar{p}$ the cross sections predicted from perturbative QCD calculations have the correct order of magnitude.

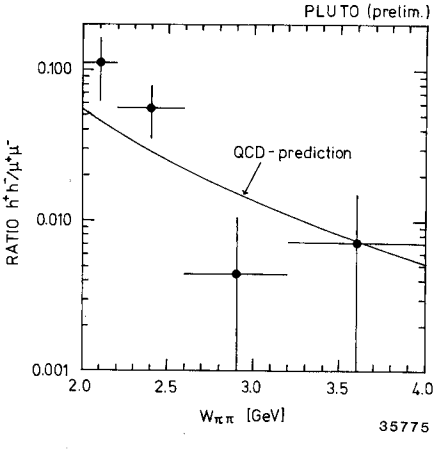

Figure 8. Ratio of two-photon production of charged hadron pairs to two-photon production of muon pairs as a function of the hadron pair mass assuming all hadrons to be pions.

3.0 TWO-PHOTON PRODUCTION OF FOUR PIONS

3.1 THE FOUR CHARGED PION FINAL STATE

The TASSO collaboration /15/ and the Mark II collaboration /16/ reported the observation of a strong enhancement in

$$\gamma\gamma \rightarrow \rho^0\rho^0 \rightarrow \pi^+\pi^-\pi^+\pi^-$$

near the $\rho^0\rho^0$ threshold. The CELLO collaboration contributed an analysis of this channel to this workshop (see below).

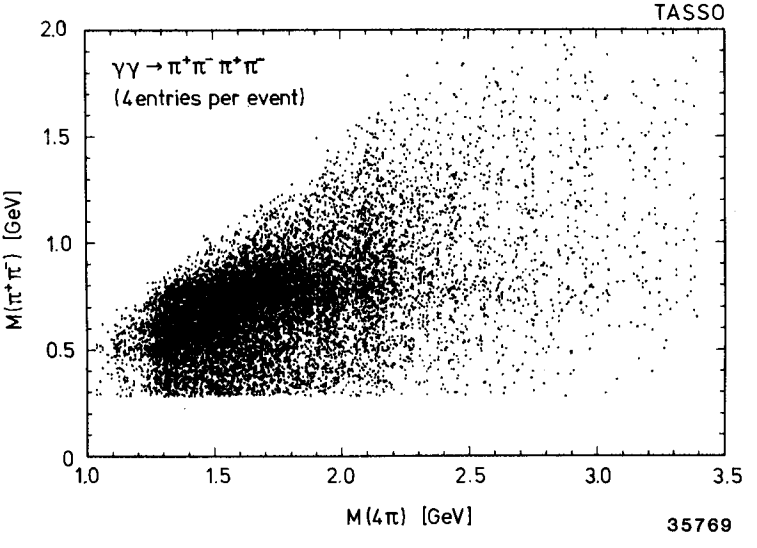

Figure 9. Plot of the masses of all $\pi^+\pi^-$ combinations versus the four pion mass in events with four charged tracks.

The evidence for the $\rho^0\rho^0$ enhancement is demonstrated in Figure 9 and Figure 10. In Figure 9 the masses of all $\pi^+\pi^-$ combinations are plotted versus the four pion mass ($M_{4\pi}$). The ρ^0 signal seems to be concentrated between $M_{4\pi}$ ~1.2 GeV and ~2.2 GeV. Figure 10 shows in two $M_{4\pi}$-bins the correlations between the corresponding pairs of $\pi\pi$ combinations, on the left for the unlike sign combinations and on the right for the like sign combinations. The $\rho^0\rho^0$ signal is clearly visible even in the lowest $M_{4\pi}$-bin between 1.3 and 1.4 GeV, although the production is considerably suppressed by phase space effects below the nominal $\rho^0\rho^0$ threshold. Possible explanations for the large $\rho^0\rho^0$ cross section near threshold have been offered by various authors in the past /17, 18, 19, 20, 21/. If the enhancement is due to resonance production, the final state would have well defined quantum numbers, like isospin, spin and parity. A check on the isospin quantum number can be made by measuring the related channel $\gamma\gamma \rightarrow \rho^+\rho^-$ as will be discussed in the next section. A spin-parity analysis has been carried out by the TASSO group by studying the angular correlations in the four pion final state.

3.1.1 Angular Correlation Analysis (TASSO)

In the no-tag case the four pion final state is defined by 7 variables. One can choose two masses (m_{12}, m_{34}), the ρ-production angle $\vartheta_\rho{}^{12}$ and two angles for each decaying ρ ($\vartheta_\pi{}^{12}$, $\varphi_\pi{}^{12}$, $\vartheta_\pi{}^{34}$, $\varphi_\pi{}^{34}$). The indices 12 and 34 refer to a pion pair as defined if one numbers the pions as follows: π^+_1, π^-_2, π^+_3, π^-_4. The rotational properties of the $\rho^\circ\rho^\circ$ system with spin-parity J^P and helicity J_z are then given by:

$$\psi^{JP,Jz} \propto \sum a_{L,Lz,S12,S34}{}^{JP,Jz}\ Y_L{}^{Lz}(\vartheta_\rho{}^{12},)\ Y_1{}^{S12}(\vartheta_\pi{}^{12},\varphi_\pi{}^{12})\ Y_1{}^{S34}(\vartheta_\pi{}^{34},\varphi_\pi{}^{34})$$

The spherical harmonics describe the ρ-production and the decay of each ρ. The coefficients $a_{L,Lz,S12,S34}{}^{JP,Jz}$ (see table in /22/) are unambiguously defined if one assumes that only the lowest multipole in the $\gamma\gamma$-system and the lowest orbital angular momentum in the $\rho^\circ\rho^\circ$-system contribute. The matrix elements for $\rho^\circ\rho^\circ$-production (without the $W_{\gamma\gamma}$-dependence) were then defined by:

$$g_{\rho\rho}{}^{JP,Jz} = 1/\sqrt{2}\ \Big(\ BW(m_{12})\ BW(m_{34})\ \psi^{JP,Jz}(\vartheta_\rho{}^{12},\vartheta_\pi{}^{12},\varphi_\pi{}^{12},\vartheta_\pi{}^{34},\varphi_\pi{}^{34})$$
$$+\ BW(m_{14})\ BW(m_{32})\ \psi^{JP,Jz}(\vartheta_\rho{}^{14},\vartheta_\pi{}^{14},\varphi_\pi{}^{14},\vartheta_\pi{}^{32},\varphi_\pi{}^{32})\ \Big)\ .$$

BW denotes the ρ Breit-Wigner amplitude. This form is symmetric with respect to the interchange of identical bosons in the final state.

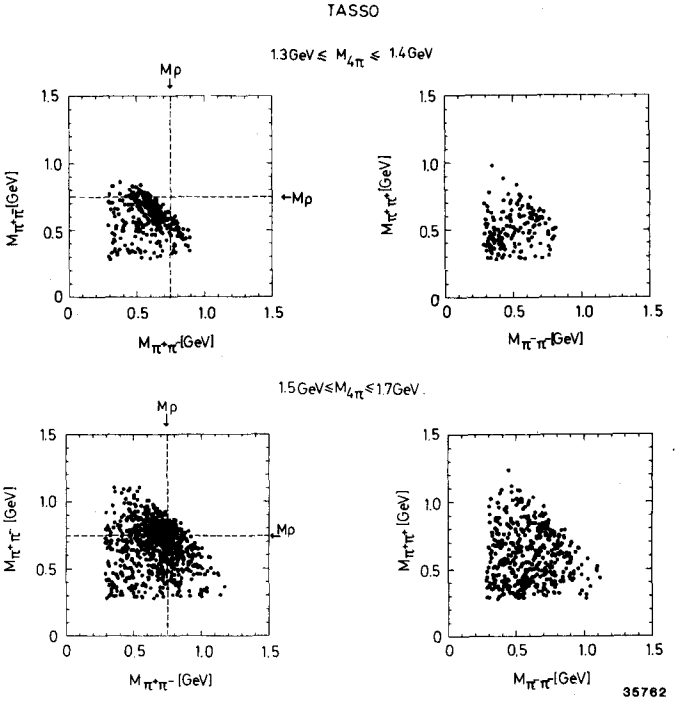

Figure 10. Plot of one $\pi\pi$ mass combination versus the other one for $\pi^+\pi^-\pi^+\pi^-$ events in two different $M_{4\pi}$ intervals; left side: $\pi^+\pi^-$ vs. $\pi^+\pi^-$; right side $\pi^-\pi^-$ vs. $\pi^+\pi^+$.

The full matrix element, i.e. including all mass and angular correlations, has been used in maximum likelihood fits for the determination of the spin-parity contributions $J^P = 0^+, 0^-, 2^+, 2^-$. The fits have been carried out in 100 MeV wide $M_{4\pi}$-bins in the range $1.2 \leq M_{4\pi} \leq 2.0$ GeV. In the fits the four charged pion yields were described by a sum of the different spin-parity states for $\rho^0\rho^0$ plus additional contributions from $\rho^0\pi^+\pi^-$ and 4π phase space. In addition to this fit with 6 parameters also a fit with 3 parameters was tried where the $\rho^0\rho^0$ contribution was described by isotropic production and decay of the ρ's.

The results of the fits presented in the following have been obtained with the full integrated luminosity collected by the TASSO experiment until summer 82 (~80 pb^{-1}). For the published data /22/ about 40 pb^{-1} were used. The new analysis was done in the same way as the published one, except for a more stringent cut in $|\sum \vec{p}_T|$ (new analysis: $|\sum \vec{p}_T| < 70$ MeV/c; old analysis: $|\sum \vec{p}_T| < 150$ MeV/c). This cut reduces the background from events with undetected particles to about 7% (before: 17%).

Figure 11a shows the $\rho^0\rho^0$ cross section obtained from the fits with isotropic $\rho^0\rho^0$ production. The data are well described by such a production mechanism. The most striking feature of the cross section is that it stays high below the nominal $\rho^0\rho^0$ threshold, although the phase space decreases drastically. That means that the matrix element has to increase steeply below threshold (see discussion in /22/).

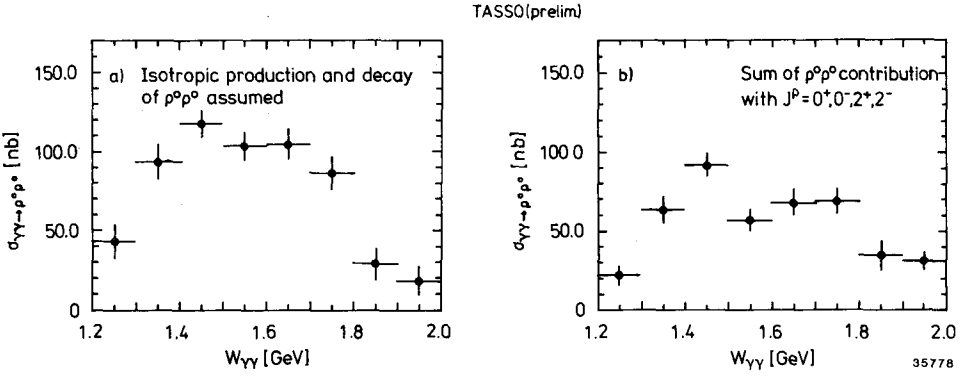

Figure 11. Cross section for $\gamma\gamma \to \rho^0\rho^0$ (TASSO): a) Isotropic $\rho^0\rho^0$ production and decay assumed; b) Sum of the contributions from $J^P = 0^+, 0^-, 2^+, 2^-$ as obtained from the fit.

Figure 11b shows the $\rho^0\rho^0$ cross section obtained by summing the different J^P-contributions determined in the fits with 6 parameters. On the average the cross section comes out somewhat lower than in the fits with isotropic $\rho^0\rho^0$ production. That has two reasons: this fit assigns less events to $\rho^0\rho^0$ (more to $\rho^0\pi^+\pi^-$) and the detection efficiency for the sum of J^P-states is different than for the $\rho^0\rho^0$ phase space. The spin-parity decomposition of the cross section is shown in Figure 12. The following conclusions can be drawn from these plots: The

spin-parity states $J^P = 0^-$ and 2^- are not dominant in the investigated $M_{4\pi}$ range. The $J^P = 0^+$ contribution is large except for the two highest $M_{4\pi}$ bins, whereas the contribution of $J^P = 2^+$ increases with $M_{4\pi}$ and is dominant in the two highest $M_{4\pi}$ bins.

Some words of caution have to be added concerning especially the region below the nominal $\rho^0\rho^0$ threshold. The results have been obtained with the special choice of the matrix elements as described above. There is no guarantee that the real world is like that. In fact, it has been reported in a parallel session at this workshop that there are indications of final state interactions at low $\rho^0\rho^0$ masses /23/. That was found by studying correlations in the $\pi\pi$-masses using TASSO data. Such final state interactions are not included in the matrix elements used in the fits.

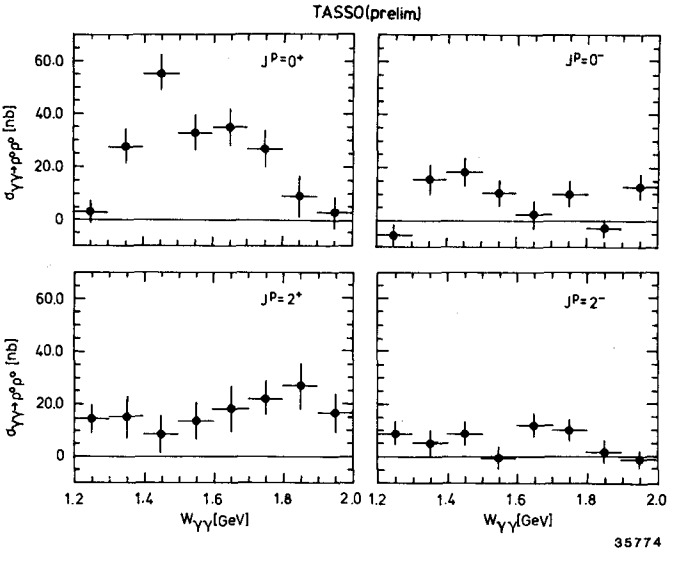

Figure 12. Decomposition of the cross section for $\gamma\gamma \to \rho^0\rho^0$ into the different spin-parity contributions (TASSO) : $J^P = 0^+$, $J^P = 0^-$, $J^P = 2^+$ and $J^P = 2^-$

3.1.2 The CELLO Analysis of $\gamma\gamma \to \pi^+\pi^-\pi^+\pi^-$

An analysis of the four charged pion final state has been presented at this workshop by the CELLO collaboration /24/. They used data from an integrated luminosity of 11.3 pb^{-1}. The event selection can be briefly summarized as follows: The selected events had to have four charged tracks with momenta $p \geq 120$ MeV/c detected in a polar angular range $|\cos\vartheta| \leq 0.95$ (TASSO: $|\cos\vartheta| \leq 0.84$). The total transverse momentum of the four pion system was required to be $|\sum \vec{p}_T| < 120$ MeV/c. After these cuts 835 events with an estimated background of 9% were found in the range $1.1 \leq M_{4\pi} \leq 2.5$ GeV.

In a first step the CELLO group determined the cross section for the production of four charged pions including possibleintermediate resonance states. To account for differences in the acceptance depending on whether resonances are formed or not, the acceptance was calculated as a function of the masses m_{12}, m_{34}, m_{14}, m_{32} of $\pi\pi$-combinations (the indices of the masses have been explained above). Since for a full determination of the system 7 variables are needed additional information from the measured angular distributions was included in the acceptance calculations. The ρ-production was assumed to be isotropic, as justified by the distribution in Figure 13a. Different decay angular distributions of the ρ's in the ρ-helicity system (Θ_π^H) were used depending on the ρ-production angle. Figure 13b shows that the decay angular distribution is flat for $|\cos\Theta_\rho| < 0.8$ and $\sim\sin^2\Theta_\pi^H$ (indicative for ρ's with helicity ±1) for $|\cos\Theta_\rho| > 0.8$. Figure 14a shows the four charged pion cross section obtained with these acceptance corrections.

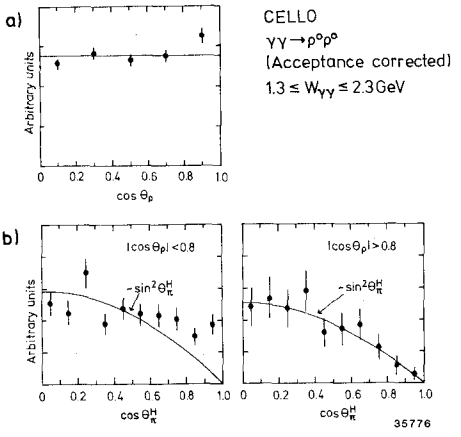

Figure 13. CELLO: Acceptance corrected angular distributions in the reaction $\gamma\gamma\to\rho^\circ\rho^\circ$ ($\rho^\circ\rho^\circ$ is defined by cuts in the $\pi^+\pi^-$ masses, $\Delta M = \pm100$ MeV) : a) Polar angular distribution of the produced ρ's w.r.t. the γ-direction in the $\gamma\gamma$ c.m.s.. b) Decay angular distribution of the ρ's in the ρ-helicity system for two $\cos\Theta_\rho$-intervals.

In a second step the CELLO group separated the three contributions $\rho^\circ\rho^\circ$, $\rho^\circ\pi^+\pi^-$ and 4π phase space in the range $1.1 \leq M_{4\pi} \leq 2.5$ GeV. For each contribution the number of events in 200 MeV wide $M_{4\pi}$-bins was determined by fitting the sum of the three contributions to the two density distributions $m(\pi^+\pi^-)$ vs. $m(\pi^+\pi^-)$ and $m(\pi^+\pi^+)$ vs. $m(\pi^-\pi^-)$.

The $\rho^\circ\rho^\circ$ cross section is shown in Figure 14a. Shape and height of the cross section are in good agreement with the TASSO result. The $\rho^\circ\rho^\circ$ channel accounts for about half the four charged pion cross section. The cross sections for $\rho^\circ\pi^+\pi^-$ and 4π phase space production are shown in Figure 14b. Note that the $\rho^\circ\pi^+\pi^-$ cross section, though of similar size, does not exhibit a threshold behaviour as dramatic as observed for $\rho^\circ\rho^\circ$, since the $\rho^\circ\pi^+\pi^-$ threshold is much lower.

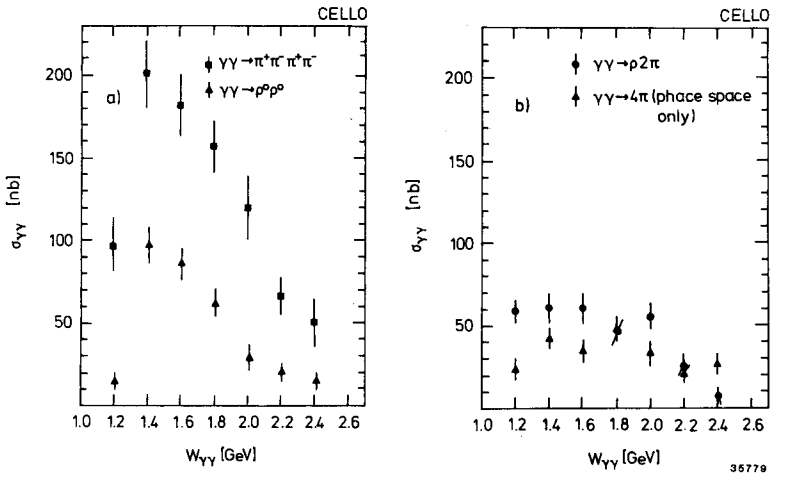

Figure 14. CELLO: a) Cross section for $\gamma\gamma \to \pi^+\pi^-\pi^+\pi^-$ (all 4 pion final states) and $\gamma\gamma \to \rho^\circ\rho^\circ$ b) Cross section for $\gamma\gamma \to \pi^+\pi^-\pi^+\pi^-$ (phase space only) and $\gamma\gamma \to \rho^\circ\pi^+\pi^-$.

3.1.3 Summary of the Results on the Four Charged Pion Final State

The results of the measurements of the four charged pion final state are: The large cross section for $\rho^\circ\rho^\circ$ production extends below the nominal $\rho^\circ\rho^\circ$ threshold. A sizeable $\rho^\circ\pi^+\pi^-$ cross section is observed. The partial wave analysis for $\rho^\circ\rho^\circ$ yields: $J^P = 0^-$ and 2^- are not dominant; $J^P = 0^+$ dominates below ~1.7 GeV and $J^P = 2^+$ above ~1.7 GeV.

What could be a possible explanation of a $\rho^\circ\rho^\circ$ enhancement with spin-parity 0^+ and 2^+ ? One interesting possibility, suggested in /20, 21/, is to explain the effect with the production of four quark bound states /25/:

$$\gamma\gamma \to q\bar{q}q\bar{q} \to \rho^\circ\rho^\circ$$

This interpretation accounts for both the threshold enhancement and for the measured spin-parity structure. The four quark states are ordered in multiplets. The lowest multiplet is a $J^{PC} = 0^{++}$ nonet with masses around 1 GeV. It has been suggested that the scalar states $\varepsilon(700)$, $S^*(980)$ and $\delta(980)$ belong into this multiplet /26, 27/. These states couple dominantly to a pair of pseudoscalar mesons (PP) and the $\gamma\gamma$-width should be suppressed (up to now in agreement with experiment). According to VMD we expect the largest couplings to $\gamma\gamma$ for the multiplets which have a dominant coupling to pairs of vector mesons (VV). Table 1 gives a summary of some expected multiplets with the average masses and the relative amplitudes for the couplings to pairs of pseudoscalar and vector mesons ('recoupling coefficients'). In general, a four quark state should be broad because it can easily decay into pairs of $q\bar{q}$ mesons. An exception could be, for example, the 0^{++}-state at about 1.45 GeV (Table 1), which couples dominantly to $\rho^\circ\rho^\circ$. This state is predicted to have a relatively narrow width (i.e. typical hadronic width)

because it lies below the threshold for its fall apart pieces ($\rho^0\rho^0$) /26/. Above threshold the widths become gradually larger.

Multiplet	$J^{PC}(I)$	Mass [GeV]	PP	VV
9*	$0^{++}(0)$	1.45	-0.177	0.644
36*	$0^{++}(0,2)$	1.80	0.041	0.743
9	$2^{++}(0)$	1.65	0	0.816
36	$2^{++}(0,2)$	1.65	0	0.577

Table 1. The recoupling coefficients of the S-wave four quark states which decay mainly into two vector mesons. P and V denote pseudoscalar and vector quark-antiquark states.

Many other explanations for the large $\rho^0\rho^0$ production have been discussed. A clue for the solution of this question is expected from measurements of the production of other vector meson pairs. Table 2 shows that different models can differ largely in their predictions for the relative yields of vector meson pair production. For the following discussion I want to emphazise that a resonance with isospin 0 decays twice as frequently into $\rho^+\rho^-$ than into $\rho^0\rho^0$.

Model	$\rho^0\rho^0$	$\rho^+\rho^-$	$\omega\omega$	$\rho^0\omega$
VMD	1	0	1/81	1/9
VMD /18/	1	-	5.8	0.5
Quark model	1	2	1	36/25
Quark model /19/	1	4/25	allowed	allowed
Resonance (I=0)	1	2	allowed	0
$qq\bar{q}\bar{q}$ /20/	1	~0	-	~1
$qq\bar{q}\bar{q}$ /21/	1	~0	0.1	0.05

Table 2. Ratios of the cross sections for $\gamma\gamma \to VV'$ to $\gamma\gamma \to \rho^0\rho^0$ as predicted from different models.

3.2 THE JADE ANALYSIS OF $\gamma\gamma \to \pi^+\pi^-\pi^0\pi^0$

The JADE group analyzed $\gamma\gamma \to \rho^+\rho^-$ studying the final state $\pi^+\pi^-\pi^0\pi^0$ in a data sample collected for an integrated luminosity of 77 pb^{-1} /28/. Events were selected requiring two charged tracks with momenta p > 100 MeV/c and four photons with shower energies E_γ > 60 MeV each. The evidence for two correlated π^0's in an event is shown in Figure 15, where one $\gamma\gamma$-mass is plotted versus the other. Photon pairs with invariant masses between 60 and 220 MeV were considered to be π^0's. For the subsequent analysis the kinematics of the two photons was fitted with a constraint on the π^0 mass.

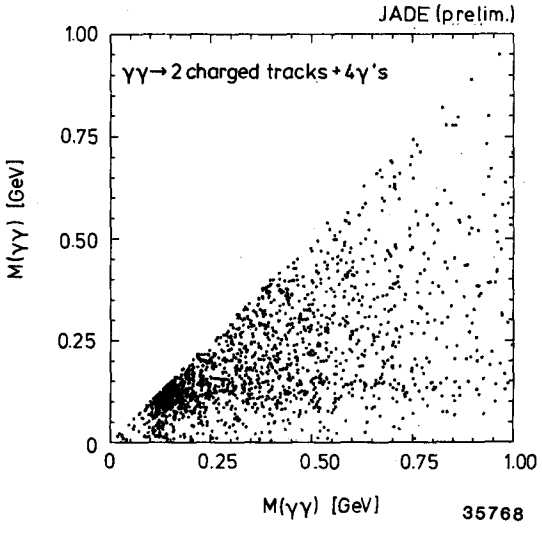

Figure 15. Plot of one $\gamma\gamma$ mass versus the other for events with 4 photons and two charged tracks detected (JADE). There are 3 entries per event.

Plotting the masses of the $\pi^+\pi^0$ and $\pi^-\pi^0$ combinations (Figure 16) one obtains a signal at the ρ-mass, which is not seen in the neutral combinations $\pi^+\pi^-$ and $\pi^0\pi^0$. The absence of a ρ° signal in the $\pi^+\pi^-$ combination is easily explained: Since the four pion final state with charge conjugation C=+1 has even isospin I, the presence of a ρ° with I=1 requires that the $\pi^0\pi^0$ combination be also in an I=1 state which is not possible for $\pi^0\pi^0$. Although there is a charged ρ signal, the two-dimensional distribution of $\pi^+\pi^0$-masses versus $\pi^-\pi^0$-masses in Figure 17a does not show a clear evidence for correlated $\rho^+\rho^-$ production. For comparison the corresponding plot for the neutral mass combinations is shown in Figure 17b.

The measured event rate as a function of the 4 pion mass is plotted in Figure 18 (open histogram). The hatched histogram is the rate restricted to the $\rho^+\rho^-$-band ($0.55 < m_\rho < 0.95$ GeV). The observed shift of the distribution after this cut may be just a phase space effect. The cross section derived from the events in the $\rho^+\rho^-$-band is plotted in Figure 19. Since the $\rho^+\rho^-$ rate has not been explicitly determined, this cross section has to be considered as an upper limit for

$\sigma(\gamma\gamma\to\rho^+\rho^-)$. The errors in the plot are statistical only; the systematic errors are on the order of 30%.

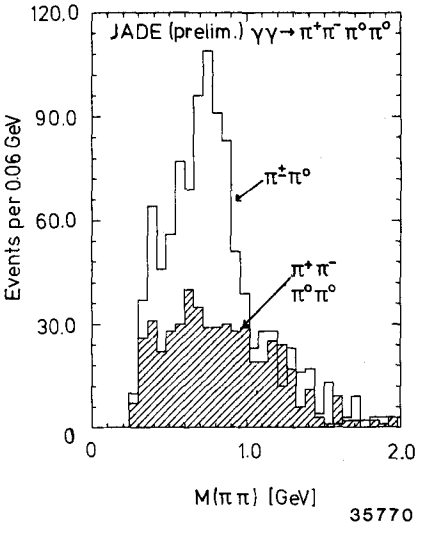

Figure 16. Mass distributions for two pion combinations in events with two charged and two neutral pions (JADE). Open histogram: charged pion pairs (4 entries per event), hatched histogram: neutral pion pairs (2 entries per event).

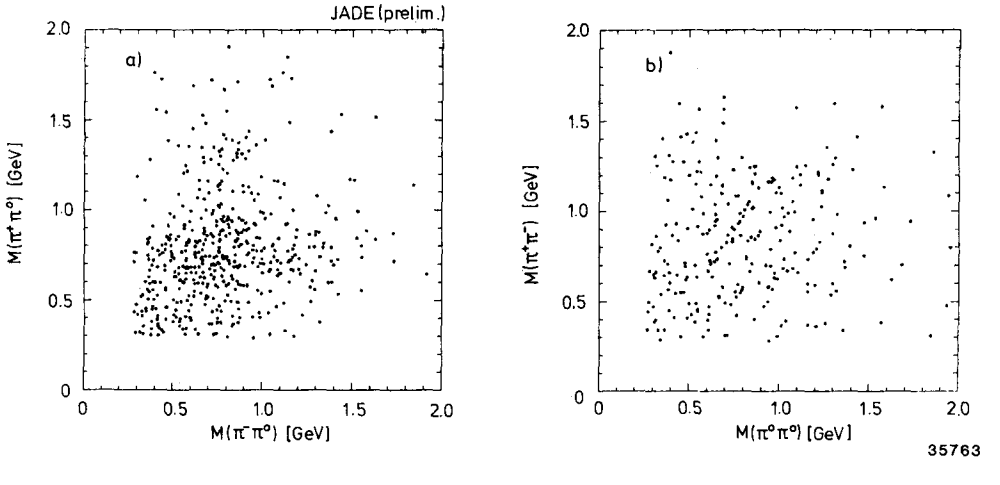

Figure 17. Two-dimensional plot of the $\pi\pi$ masses shown in Figure 16 (JADE). (a: charged pion pairs, 2 entries per event; b: neutral pion pairs, 1 entry per event).

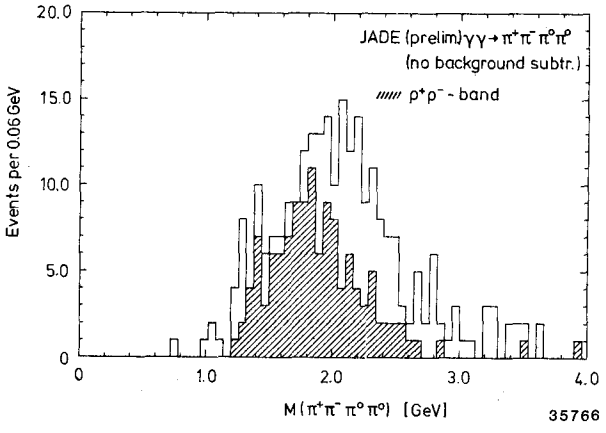

Figure 18. Four pion mass spectrum of the reaction $\gamma\gamma \to \pi^+\pi^-\pi^0\pi^0$ (JADE). The hatched histogram is the same spectrum with mass combinations in the $\rho^+\rho^-$ band.

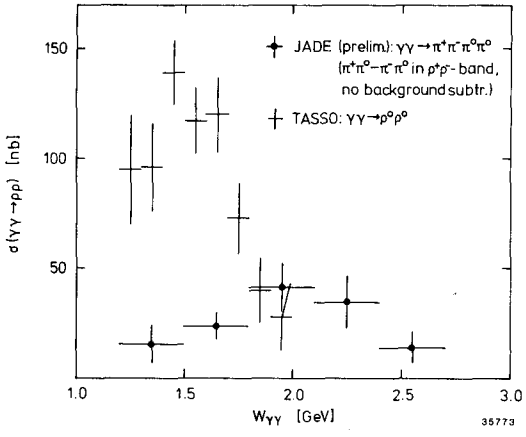

Figure 19. Cross section for $\gamma\gamma \to \rho^+\rho^-$ obtained from the hatched histogram in previous figure (JADE, preliminary). Also shown is the cross section for $\gamma\gamma \to \rho^0\rho^0$ from TASSO /22/.

A comparison of this cross section with the $\rho^0\rho^0$ cross section shows very clearly that both cross sections have a totally different behaviour at threshold. That means in particular that the $\rho^0\rho^0$ enhancement cannot be due to a single resonance with well defined isospin. The relative rates expected for the decay of a resonance with isospin I (I = 0, 2) into pairs of neutral and charged ρ's are:

I	$\rho^+\rho^-$	$\rho^\circ\rho^\circ$
0	2	1
2	1	2

Which possibilities are now remaining for the explanation of the $\rho^\circ\rho^\circ$ enhancement? Models, which are related to VMD, will always prefer $\rho^\circ\rho^\circ$- over $\rho^+\rho^-$-production and thus conform with the measurements. The four-quark models of /20/ and /21/[1] also predict a small $\rho^+\rho^-$ cross section due to interferences between different states.

3.3 OBSERVATION OF A NARROW STRUCTURE AT 2.1 GEV IN $\gamma\gamma\to\pi^+\pi^-\pi^+\pi^-$

The TASSO collaboration observed a narrow structure around 2.1 GeV in the four charged pion mass spectrum (Figure 20) /29/. A smooth curve was fitted to the mass spectrum between 1.65 and 3.0 GeV including the signal region. For masses between 2.05 and 2.15 GeV the observed event rate is 4.3 standard deviations larger than expected from this fit. Including a Breit-Wigner function in addition to the smooth curve the fit gives a good description of the data and yields for the Breit-Wigner parameters, mass and width, and for the number of events in the peak:

$$M=2.103\pm0.01\ \text{GeV}, \quad \Gamma=0.030\pm0.034\ \text{GeV}, \quad N=125.6\pm46$$

In this fit the 4 pion mass resolution, which is about 60 MeV (FWHM) near 2 GeV, has been taken into account. If this structure is indeed a resonance its $\gamma\gamma$ coupling is:

$$\Gamma_{\gamma\gamma}\cdot(2J+1)\cdot B(4\pi^\pm) = 1.25 \pm 0.5\ (\text{stat.}) \pm 0.5\ (\text{syst.})\ \text{keV}$$

J is the spin of the resonance and $B(4\pi^\pm)$ the decay branching ratio into four charged pions. Upper limits for the branching ratios into $\rho^\circ\rho^\circ$ and $K_0\bar{K}_0$ are found to be

$$B(\rho^\circ\rho^\circ)/B(4\pi^\pm) < 0.6\ (95\%\ \text{c.l.}),$$
$$B(K_0\bar{K}_0)/B(4\pi^\pm) < 0.06\ (95\%\ \text{c.l.}).$$

The signal does not seem to be correlated with the large $\rho^\circ\rho^\circ$ enhancement observed between threshold and $M_{4\pi} \sim 2$ GeV. Removing events which have a $\pi^+\pi^-$-$\pi^+\pi^-$ combination in the $\rho^\circ\rho^\circ$-band (cut in the ρ°-mass: ±150 MeV) the $M_{4\pi}$ distribution in Figure 21a was obtained. Although the signal appears more pronounced in this plot a quantitative analysis is more difficult because the effect of the applied cut on the background introduces uncertainties. The signal to back-

---

[1] At the time of the workshop there was a discrepancy between the predictions for the $\rho^+\rho^-$ cross section from /20/ and /21/. Meanwhile the authors of /21/ corrected their calculations.

ground ratio is improved if one plots only events which appear planar in the laboratory system (Figure 21b). "Planar" is defined by $Q_1 < 0.05$, where Q_1 is the smallest eigenvalue of the sphericity tensor. Monte Carlo studies showed that the latter cut also enhances 4π phase space over $\rho^0\rho^0$ final states. The effects of these kinematical cuts are still under study by the TASSO group.

If the observed narrow structure will be confirmed as a resonance it cannot easily be associated with a known state with similar resonance parameters. The nearest candidate would be the h(2040), but it does not seem to have the same resonance parameters. Note however, that the authors of /30/ predicted a relatively large $\gamma\gamma$-width for the h(2040), which they called in the paper the f^0-recurrence f*.

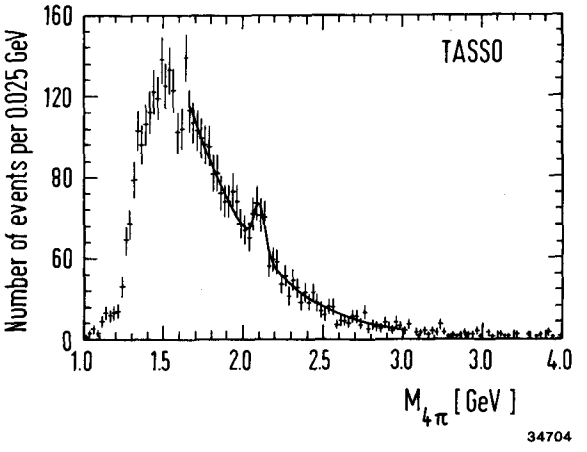

Figure 20. Four charged pion mass spectrum (TASSO).

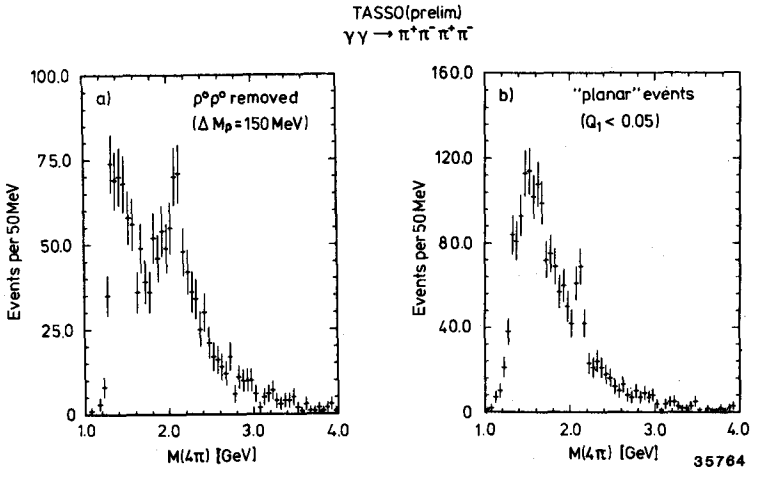

Figure 21. Four charged pion mass spectrum (TASSO): a) $\rho^0\rho^0$ events removed; b) events with $Q_1 < 0.05$

4.0 THE TOTAL CROSS SECTION FOR TWO-PHOTON PRODUCTION OF HADRONS AT LOW Q^2

4.1 EXCLUSIVE FINAL STATES AND THE TOTAL CROSS SECTION

The large amount of experimental results on exclusive final states in two-photon scattering enables us to compare the exclusive measurements with the experimental determinations of the total $\gamma\gamma$ cross section and theoretical expectations.

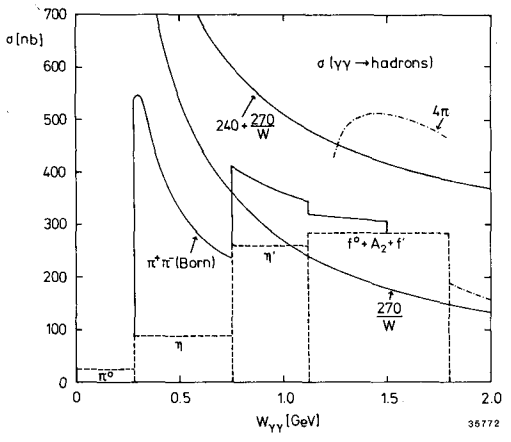

Figure 22. Sum of measured $\gamma\gamma$ cross sections compared to predictions from Regge model calculations /31/. The sum of cross sections includes resonance production, the Born cross section for $\gamma\gamma \to \pi^+\pi^-$ and 4 pion production, $\gamma\gamma \to \pi^+\pi^-\pi^+\pi^-$ and $\gamma\gamma \to \pi^+\pi^-\pi^0\pi^0$ (restricted to $\rho^+\rho^-$-band).

In Figure 22 the measured exclusive channels are summed up. The resonances are schematically represented by rectangular boxes with areas equal to those under the corresponding resonance curve. The $\pi^+\pi^-$ continuum was assumed to be represented by the Born approximation up to 1.5 GeV. The curve for four pion production includes the four charged pion production cross section taken from Figure 14 (CELLO) and the $\gamma\gamma \to \pi^+\pi^-\pi^0\pi^0$ cross section (restricted to the $\rho^+\rho^-$-band) from Figure 19 (JADE).

The measured exclusive cross sections are compared to estimates using the Regge model. Relating $\gamma\gamma$ scattering to γ-nucleon and nucleon-nucleon cross sections at high energies the $\gamma\gamma$ total cross section was predicted to be /31/:

$$\sigma_{\gamma\gamma} = (240 + 270/W) \text{ nb} \quad (W \text{ in GeV}).$$

The constant term accounts for pomeron exchange and the 1/W-term arises from the leading Regge trajectories (f^0, A_2). Contributions from non-leading Regge trajectories (like the f'-trajectory) giving rise to terms with higher powers in 1/W were estimated to be small. Via duality the 1/W-term should reproduce the aver-

age of the resonance cross sections. In fact, the measured resonances seem to saturate roughly this predicted cross section (Figure 22).

On the other hand, it has been suggested that in addition to the Regge contributions there may be non-Regge terms arising from the pointlike coupling of the photon. According to /32/ a rough estimate for this contribution could be the simple quark loop box diagram. That would add a term $\sim 1/W^2$ to the total cross section. In /32/ it was argued that such an additional term was needed to account for the resonance contributions, which had been estimated using superconvergent sum rules. Now the measured cross sections for the resonances show that this argument is no longer valid. The superconvergent sum rule discussed in /32/ requires a $\gamma\gamma$-width of the f^0 of ~9 keV, which has to be compared to the measured value of ~3 keV (see also discussion in /33/). One may wonder if this too large estimate is caused by the assumption that below ~2 GeV the total cross section is saturated by resonances (i.e. the pseudoscalar, scalar and tensor $q\bar{q}$-resonances). Does the discrepancy between the predicted and the measured $\gamma\gamma$-width of the f^0 mean that there must be additional production of 2^+-states? For example, what is the role of four-quark states, in the estimates of resonance cross sections via duality arguments as done in /31/? Since a lot of experimental results on $\gamma\gamma$ resonance production and other exclusive final states are now available, these questions should be reinvestigated.

4.2 THE EXPERIMENTAL DETERMINATION OF THE TOTAL HADRONIC CROSS SECTION

Measurements of the $\gamma\gamma$ total cross section have a major disadvantage compared to the measurements of the one-photon annihilation cross section: The center-of-mass energy, $W_{\gamma\gamma}$, of an event is not known because the photons provide a continuous spectrum of $W_{\gamma\gamma}$-values. Hence $W_{\gamma\gamma}$ has to be measured. In a double-tag experiment $W_{\gamma\gamma}$ is in principle determined by the measured kinematics of the scattered leptons. But it is difficult to obtain sufficient resolutions in the tagging devices. For typical forward detectors at PETRA and PEP the resolution is not good enough for measuring the total cross section in the resonance region. In the single-tag or no-tag case $W_{\gamma\gamma}$ has to be reconstructed from the measured hadrons. Because of the imperfect detection the measured $W_{\gamma\gamma}$ (W_{vis}) will in general be smaller than the real $W_{\gamma\gamma}$. The determination of the $W_{\gamma\gamma}$ dependence of the cross section therefore requires the use of a model, which realistically describes the hadronic final states. The ingredients of such models are for example:

- a multibody phase space with limited transverse momenta of the particles w.r.t. the direction of the photons (p_T), $d\sigma/dp_T^2 \sim \exp -ap_T^2$ or $\sim \exp -bp_T$;
- the average multiplicities as a function of $W_{\gamma\gamma}$ for different particle species (charged and neutral π's, K's, ρ's,...);
- multiplicity distributions;
- the Q^2-dependence of the cross section.

The Q^2-parametrization is also needed for the extrapolation to the cross section for real photons. In Figure 23 the dependence of the cross section on Q^2 obtained from simple ρ-pole dominance is compared to the expectation from a generalized vector meson dominance model (GVMD) /34/. For the Q^2 range covered by typical small angle taggers the change in the extrapolated cross section is about 30 to 50% in the single-tag case.

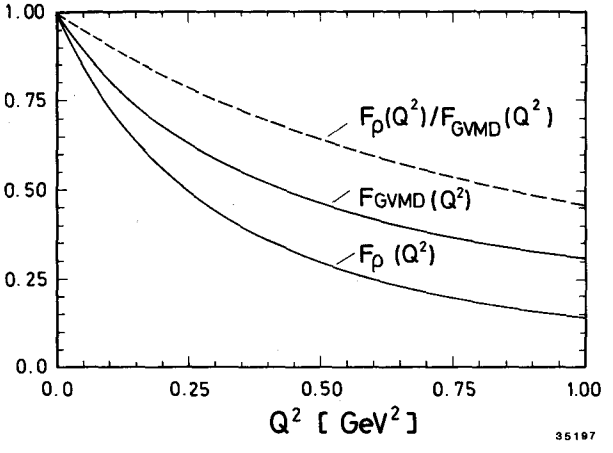

Figure 23. Q^2 dependence of the two-photon cross section for ρ-pole dominance and GVMD. The dashed curve is the ratio of both (F_ρ/ F_{GVMD}).

There have been two early analyses of the total cross section using the single tag method: the published analysis of the PLUTO group /35/ and a preliminary analysis of the TASSO group /36/. The discrepancies between both analyses, especially in the low $W_{\gamma\gamma}$ region, have been often discussed in the past. At low $W_{\gamma\gamma}$ the PLUTO group found a steep increase of the cross section described by a large coefficient of the $1/W^2$-term in a parametrization of the cross section according to:

$$\sigma_{\gamma\gamma} = A + B/W + C/W^2$$

In the preliminary TASSO analysis the inclusion of a $1/W^2$-term was not necessary.

To understand the reason for this discrepancy the TASSO group carried out a detailed study of the model dependence of the total cross section determination /37/. This study was done with data corresponding to an integrated luminosity of ~9 pb^{-1}, which is about 3 times the amount available for the previous analysis. Events with at least 3 charged tracks were selected for the analysis; neutral energy measurements were not available for these data.

With these data an attempt was made to fit simultaneously the model parameters, such as the p_T-slope, the average charged multiplicity and the different cross section terms, by comparing experimental distributions to the Monte Carlo generated distributions. For this purpose a method was developed which supplied the con-

tents of the Monte Carlo distributions as continuous functions of the parameters. This procedure allows one to study the correlations between the parameters.

The result of the fits was rather disappointing: The correlations between the parameters turned out to be so large that a reliable unfolding of the $W_{\gamma\gamma}$ distribution was not possible. The stability of the fit could be improved if some of the parameters, like the p_T-slope and the multiplicity, were fixed. But this approach is of questionable validity since these parameters are in principle unknown.

This study was done with a specific detector. It is clear that a higher detection efficiency for both charged and neutral particles will improve the results of the unfolding procedure. However, some conclusions are of more general validity: The study has shown that the determination of the total cross section is more complicated than assumed in the first analyses. Only a simultaneous fit of all model parameters can reveal correlations and allows to prove the significance of a result for the W-dependence of the cross section. The significance of the result is considerably increased if one can show that all distributions, especially the p_T and the multiplicity distributions, are equally well described for all W_{vis} values. In particular, the determination of the p_T-slope before the proper unfolding, without regarding correlations with other parameters and averaging over all W_{vis} values, was found to be dangerous.

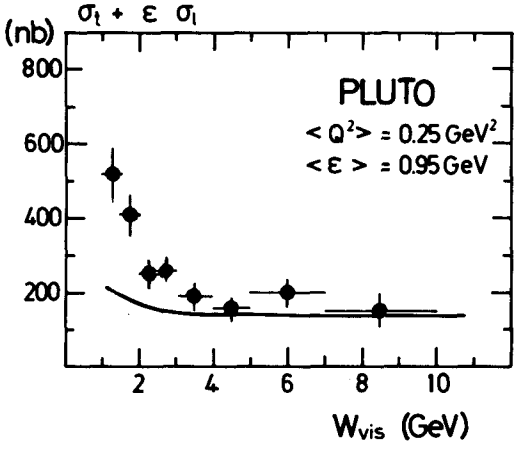

Figure 24. The total cross section versus the visible invariant mass (Pluto): $\sigma_{TT} + \varepsilon\sigma_{LT}$ at $\langle Q^2 \rangle = 0.25$ GeV^2. The prediction of the Regge estimate is given by the solid curve.

The determination of the cross section below $W_{\gamma\gamma} \sim 2$ GeV is particularly difficult (see also the discussion in /38/). Figure 24 demonstrates that the large $1/W^2$-term in the cross section found by the PLUTO group is required only by the data points below $W_{\gamma\gamma} \sim 2$ GeV. However, in the resonance region one has to expect special problems: The acceptance for events below 2 GeV is only ~8% /38/. On the other hand, about 85% of the events observed at $W_{vis} < 2$ GeV come from higher $W_{\gamma\gamma}$ values due to smearing /39/. In such a situation the cross section cannot be

obtained applying simple acceptance corrections as it was done in Figure 24, where the cross section is given as a function of W_{vis}. A proper unfolding procedure is necessary as described e.g. in /37/. Concerning the applicability of the used model to the resonance region, one has to question whether a multi-pion phase space model with limited p_T and some statistical multiplicity distribution works well for resonances. Another uncertainty has been mentioned in /38/: At low $W_{\gamma\gamma}$ the Q^2 extrapolation to $Q^2=0$ is especially large, about a factor 3 in the PLUTO analysis.

My personal conclusion is that the total hadronic cross section for two real photons below $W_{\gamma\gamma} \approx 2$ GeV is not yet known. A similar conclusion was drawn by Ch.Berger at the Paris meeting /38/.

New results are expected from JADE, the improved PLUTO detector and the PEP4/PEP9 experiment. Recently, the ARGUS collaboration proposed the installation of a 0°-tagger at DORIS /40/. This device is supposed to achieve a resolution good enough to measure the total cross section down to the resonance region in a double-tag experiment.

5.0 SUMMARY

HADRON PAIR PRODUCTION. The $\pi^+\pi^-$ continuum seems to be well approximated by the Born term up to the f^0 region. To search for scalar resonances below 1 GeV one should look for deviations from the Born cross section. The charged hadron pair production above 2 GeV is roughly in agreement with absolute QCD calculations for pion, kaon and proton pairs. Differential cross sections for $\gamma\gamma \to p\bar{p}$ for $2.0 < M(p\bar{p}) < 3.1$ GeV have been presented.

FOUR PION PRODUCTION. The most interesting new result on this reaction: The strong $\rho^\circ\rho^\circ$ threshold enhancement has no counterpart in $\rho^+\rho^-$. That excludes an interpretation of the $\rho^\circ\rho^\circ$ enhancement as one single resonance. A partial wave analysis of $\rho^\circ\rho^\circ$ yielded large $J^P = 0^+$ intensities below ~1.7 GeV and $J^P = 2^+$ intensities above ~1.7 GeV. A four-quark model predicts roughly this structure. The narrow structure observed in the four charged pion mass spectrum around 2.1 GeV waits for confirmation by other experiments.

THE TOTAL TWO-PHOTON CROSS SECTION. The measured resonances are approximately in agreement with the estimated contributions from leading Regge trajectories. Some inconsistencies between sum rule results for resonance production by two photons and the now available measurements have been pointed out. Future analyses of the total cross section will show whether the experimental problems, which have been encountered in the past with unfolding the W_{vis} distribution, can be overcome.

I am indebted to many collegues for valuable discussions and support in preparing this talk. In particular, I want to mention here: H.J.Behrend, Ch.Berger, S.Cooper, E.Hilger, R.Kellogg, L.Köpke, H.Kück, J.Olsson, W.Wagner, R.Wedemeyer, N.Wermes and M.Wollstadt. I would like to thank the organizers of the workshop for an extremely pleasent atmosphere in and around the workshop.

REFERENCES

/1/ TASSO Collaboration, M.Althoff et al., Phys.Lett. 121B (1983) 216;
/2/ G.Mennessier, Z.Phys. C16 (1983) 241
/3/ A.Courau et al., Phys.Lett. 96B (1980) 402;
R.Wedemeyer, Proc. of the Intern. Symposium on Lepton and Photon Interactions at High Energies, Bonn, 1981 and paper No.48 submitted to the conference
/4/ A.Courau, private communication
/5/ V.M.Budnev et al., Phys.Rep. 15 (1975) 181
/6/ A.Roussarie et.al., Phys. Lett. 105B (1981) 304
/7/ F.Kovacs (CELLO), presented at the experimental parallel session at this workshop
/8/ TASSO Collaboration, R.Brandelik et al., Phys. Lett. 108B (1982) 67
/9/ H.Kück (TASSO), presented at the experimental parallel session at this workshop
/10/ N.Arteaga-Romero, Seminar on $\gamma\gamma$-Physics, LPC/82-14, Paris (1982)
/11/ P.H.Damgaard, Nucl.Phys. B211 (1983) 435.
/12/ G.P.Lepage and S.J.Brodsky, Phys.Rev. D21 (1980) 2157
/13/ R.Kellogg (PLUTO), presented at the experimental parallel session at this workshop
/14/ PLUTO Collaboration, Ch.Berger et al., Nucl.Phys. B202 (1982) 189
/15/ TASSO Collaboration, R.Brandelik et al., Phys.Lett. 97B (1980) 448
TASSO Collaboration, M.Althoff et al., Z.Phys. C16 (1982) 13
/16/ D.L.Burke et.al., Phys. Lett. 103B (1981) 153
/17/ J.Layssac and F.M.Renard, Montpelier preprint PM/80/11 (1980)
H.Goldberg and T.Weiler, Phys. Lett. 102B (1981) 63;
R.M.Godbole and K.V.L.Sarma, Phys. Lett. 109B (1982) 504;
S.Minami, Lett. Nuov. Cim. 34 (1982) 125;
/18/ G.Alexander, U.Maor and P.Williams, Phys.Rev. D26 (1982) 1198
/19/ K.Biswal and S.P.Misra, Phys.Rev. D26 (1982) 3020
/20/ N.N.Achasov, S.A.Devyanin, and G.N.Shestakov, Phys. Lett. 108B (1982) 134; Z.Phys. C16 (1982) 55;
/21/ Bing An Li and K.F.Liu, Phys.Lett. 118B (1982) 435 and Erratum, Phys.Lett. 124B (1983) 550.
/22/ TASSO Collaboration, M.Althoff et al., Z.Phys. C16 (1982) 13
/23/ A.Shapira (TASSO), presented at the experimental parallel session at this workshop
/24/ H.J.Behrend (CELLO), presented at the experimental parallel session at this workshop
/25/ R.L.Jaffe, Phys.Rev. D15 (1977) 267 and 281;
R.L.Jaffe and K.Johnson, Phys.Lett. 60B (1976) 201
/26/ M.S.Chanowitz, Lectures given at the SLAC Summer Institute 1981
/27/ L.Montanet, Rep.Prog.Phys. 46 (1983) 337
/28/ J.Olsson (JADE), presented at the experimental parallel session at this workshop
/29/ D.Lüke, XXI International Conference on High Energy Physics, Paris(1982);
H.Kolanoski, Proc. of the Seminar on $\gamma\gamma$ Physics, Montpellier, Dec. 9-10, 1982
/30/ B.Schrempp et al., Phys.Lett. 36B (1971) 463.

/31/ J.L.Rosner, Brookhaven report CRISP 71 26 (1971)
/32/ M.Greco and Y.Srivastava, Nuovo Cim. 43A (1978) 88;
M.Greco, Talk given at the International Workshop on $\gamma\gamma$-Collisions (Amiens), Lecture Notes in Physics No 134, Springer (1980)
/33/ J.Field, Proc. of the Seminar on $\gamma\gamma$ Physics, Montpellier, Dec. 9-10, 1982
/34/ I.F.Ginzburg and V.G.Serbo, Phys.Lett. 109B (1982) 231
/35/ PLUTO Collaboration, Ch.Berger et al., Phys.Lett. 89B (1981) 287
F.A.Raupach, Thesis, DESY PLUTO 81/10 (1981)
/36/ E.Hilger, Talk given at the International Workshop on $\gamma\gamma$-Collisions (Amiens), Lecture Notes in Physics No 134, Springer (1980)
W.Hillen, Thesis Bonn 1981, BONN-IR-81-7
/37/ N.Wermes, Thesis Bonn 1982, BONN-IR-82-27;
N.Wermes (TASSO), presented at the experimental parallel session at this workshop
/38/ Ch.Berger, Talk given at the 4th Internat. Coll. on $\gamma\gamma$-Interactions, Paris 1981
/39/ W.Wagner, private communication
/40/ ARGUS Collaboration, Proposal to DESY-PRC 1983/06

DISCUSSION

Q: Ch.Berger (Aachen): You said, σ_{TOT} is not known yet, i.e. the PLUTO experiment is wrong. Does this statement come from a new analysis or new experimental facts ?

A: H.K.: I concluded that the cross section below 2 GeV is not yet known. I cannot prove that the PLUTO experiment is wrong, but I think PLUTO cannot prove that their result is right.

C: Ch.Berger (Aachen): One can get rid of false experiments in two ways: a) finding a bug in the analysis, b) presenting a new and better experiment but not by digging out an old experiment which is in every respect worse than the PLUTO experiment.

A: H.K.: One should also be allowed to criticize an experiment if one finds problems in the analysis. We want to learn to do better.

Q: J.Kovacs (Paris): On Greco's superconvergent sum rules which I discussed in a parallel session: The expression assumes resonance saturation and this is obviously not true if you look at the CELLO results of dipions in the f^0 region. But is it possible to theorists to formulate another expression relating cross sections with helicity 2 and 0 and taking into account the continuum?

C: P.Singer (Technion): I would like to make two remarks: 1) From the small ratio of the $\gamma\gamma \to \rho^+\rho^-$ versus $\gamma\gamma \to \rho^0\rho^0$ it is too early to conclude that a certain model, like the four-quark model, is successful. There are several models anticipating this effect, some which you have not mentioned. For instance, η exchange in $\gamma\gamma \to \rho^0\rho^0$ was calculated by using the experimental $\rho \to \eta\gamma$ width by C.Schmidt from ETH (unpublished) and I understand this could be a significant contribution.

2) You mentioned trouble with sum rules in relation with $T \to \gamma\gamma$ widths. It seems to me that this is specific to superconvergent $\gamma\gamma$ scattering sum rules (due to Greco and Grassberger and Kögerler). However, there is no similar problem if one considers the pseudoscalar meson - photon scattering amplitudes, from which the correct A_2, f^0, $f' \to \gamma\gamma$ widths were derived. I discussed this topic in the theoretical session.

Q: S.Brodsky (Stanford): Have you compared the $\gamma\gamma \to \rho^0\rho^0$ data with the QCD prediction at large mass ? The QCD predictions give significantly larger cross sections for $\rho\rho$ compared to $\pi\pi$ and have definite ρ-helicity and angular behaviours.

A: H.K.: As far as I know that has not yet been done.

Q: U.Maor (Tel-Aviv): Concerning the $\gamma\gamma \to \rho^0\rho^0$ data, I think that the first question to be asked is if the threshold enhancement observed is particular to $\gamma\gamma$ or just a phenomenon compatible with the rest of our knowledge on two-body cross sections near threshold coupled with the particular $\gamma\gamma$ kinematics. The conclusion of Alexander, Williams and myself is that apparently the $\rho^0\rho^0$ enhancement does not require any "exotic" explanation. In general, I suggest that data analysis advocating some "new physics" explanation should secure that the ratio of the "new physics" signal to the "old physics" background is good enough to make such an analysis sensible.

A: H.K.: I do not think that relating the $\rho^0\rho^0$ production to other processes via VMD-Regge helps one to understand the underlying physics of the effect.

Q: B.Stella (Rome): Could you comment somewhat more on the 2.1 GeV effect? I think that TASSO has now enough statistics to show some dynamical effect,

like angular dependences, in order to exclude the interpretation of 2.1 being a kinematical (?) effect.

A: H.K.: The analysis of the narrow structure around 2.1 GeV includes all the data TASSO collected up to summer 82. The angular distributions do not show any special behaviour in the signal region. There is one property which seems to distinguish the signal from background: The events in the signal region look flatter than the events in the sidebands. Monte Carlo studies showed that this behaviour is expected if the signal is predominantly due to four pion phase space production rather than $\rho^{\circ}\rho^{\circ}$. It has also been checked that there are no obvious signals in other channels (but upper limits have not yet been evaluated).